

4

AD FILE COPY

AD-A203 944

DEVELOPMENT OF A PLASMA PINCH PHOTOCATHODE
FINAL REPORT

1 SEPT. 1985 TO 31 DEC. 1987

FOR
OFFICE OF NAVAL RESEARCH
800 NORTH QUINCY STREET
ARLINGTON, VA 22217-5000

CONTRACT: N00014-85-K-0598

DTIC
ELECTRONIC
FEB 14 1988
D

BY
JOHN F. ASMUS
INSTITUTE FOR PURE AND APPLIED PHYSICAL SCIENCES, Q-075
UNIVERSITY OF CALIFORNIA, SAN DIEGO
LA JOLLA, CA 92037

DEPARTMENT OF THE ARMY
AGENCY USE ONLY

CONTENTS

1.0 INTRODUCTION.....3
2.0 PINCH PHOTOCATHODE STATUS.....5
3.0 PUBLICATIONS.....16



Accession For	
NTIS CRA&I	<input checked="" type="checkbox"/>
DTIC TAB	<input type="checkbox"/>
Unannounced	<input type="checkbox"/>
Justification	
By <i>per NP</i>	
Dist	
Availability Codes	
Dist	Availability Codes
<i>A-1</i>	

1.0 INTRODUCTION

For the past two years this project has focused on developing a high-current photocathode technology for advanced LINACS such as ETA and ATA. The need is for a high-performance (emittance, current, and life) cathode that will not poison in the only moderately good vacuums of such systems. Our approach embodies the durability of an unsensitized metal photocathode that is illuminated by a high-Z, high-density plasma pinch formed from a liquid-jet source in vacuum. The principal advantage of this pinch over a laser is both its simplicity and its ability to efficiently produce high-power vacuum ultraviolet radiation.

The present laboratory pinch photocathode is operating with a decane jet and a copper cathode. The peak pulse power exceeds 100 MW at a repetition rate of 10Hz. Photoelectron current densities as high as 60 A/sq cm have been attained in microsecond pulses. At this point we feel that it would be appropriate to advance to the next order of technical issues pertaining to the incorporation of the device into an operating LINAC and determining cathode life in such an environment.

A convenient and cost-effective opportunity has emerged for mounting a full-scale demonstration and evaluation of the pinch photocathode. Maxwell Laboratories of San Diego has begun assembling a clone of an ETA module which will be available for experiments by May 1988. Thus, we look forward to adapting the pinch photocathode system to the ETA configuration and evaluating its performance on the nearby system at Maxwell. From this we will be able to measure beam emittance and cathode life on an operating induction LINAC. These data will be available then to

the ATA effort for comparison with the results from the thermionic dispenser cathode program that is presently underway. If the thermionic route encounters cathode poisoning difficulties, the pinch photocathode may then offer an attractive alternative with minimal lead time to installation on ATA. Irrespective of the poisoning issue, there is reason to believe that the pinch photocathode will produce a low-emittance electron beam at higher current densities than possible with a thermionic cathode. Thus, the pinch photocathode may prove to be of considerable importance in the scaling of FELs to higher powers.

The next two sections describe the status of the present rep-rate photocathode and our proposal to install it on the ETA induction LINAC module, respectively.

2.0 PINCH PHOTOCATHODE STATUS

During the past year the laser-guided gas-embedded pinch vacuum-ultraviolet source was converted to a liquid-jet configuration in vacuum. This was undertaken for several reasons. First, the necessity of interposed high-density background gas is avoided. Second, a channel-forming guide laser beam is no longer needed. Finally, a wide variety of high-Z low-cost substances are available in liquid form. For these reasons the liquid-jet approach makes sense for a rep-rate version of the pinch illuminator. Background gas absorption of hard UV is lessened. A large gas-transport system is not needed. Radiation output may be optimized through selection of the liquid's vapor pressure, surface tension, density, and composition.

The present laboratory experimental pinch photocathode apparatus is pictured in Figure 1 and illustrated schematically in Figure 2. In the right foreground of Figure 1 are the coax inductors emerging from the PFN, below. They attach to the center electrode of the spark-gap switch. The liquid-jet pinch chamber is in the center and the liquid enters from the electrical valve at the top center. The cryogenic apparatus that effects the condensation of the fluid is at the left. Optical and electrical diagnostic instruments surround the perimeter of the pinch tube. The liquid-jet nozzle is a stainless steel insert within the pinch-discharge cathode (Mallory metal). Its flow aperture has a diameter of 100um. Figure 2 illustrates the overall arrangement in a highly schematic and simplified form (but drawn reversed, left to right, from the perspective of Figure 1). In Figure 2 the pinch discharge cathode is located at the intersection of the UV

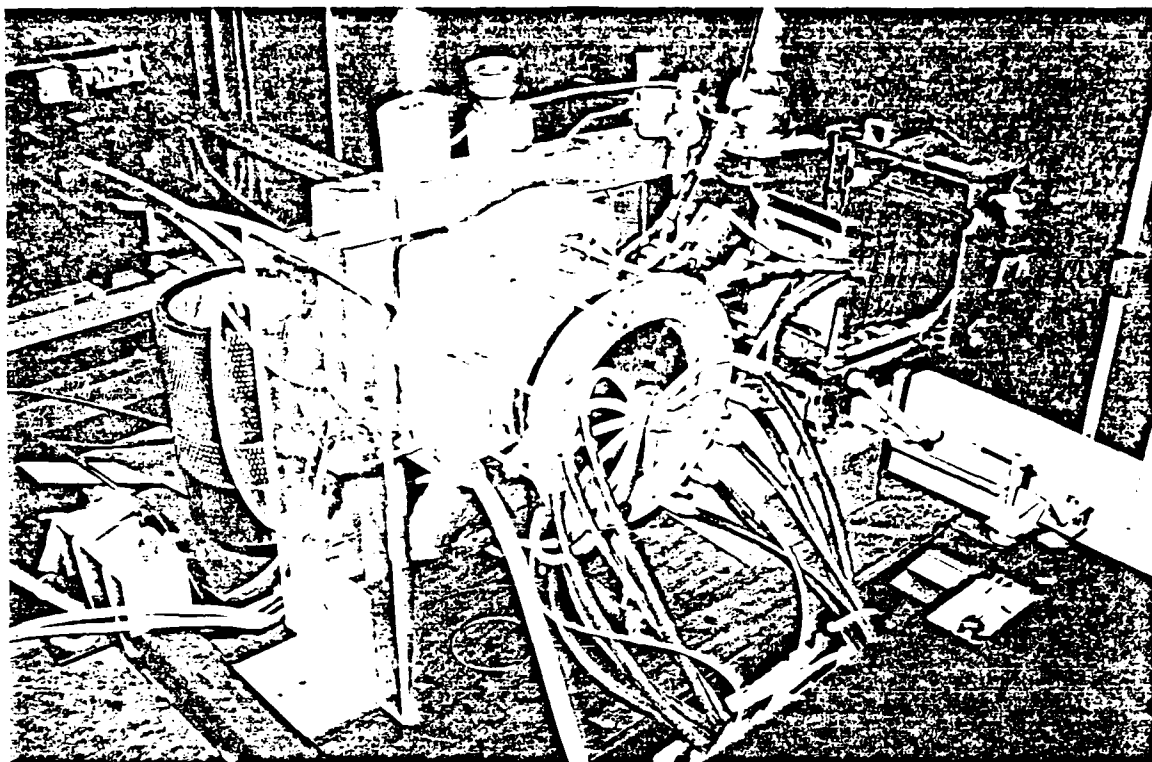


FIGURE 1. Photograph of the liquid-jet pinch photocathode device.

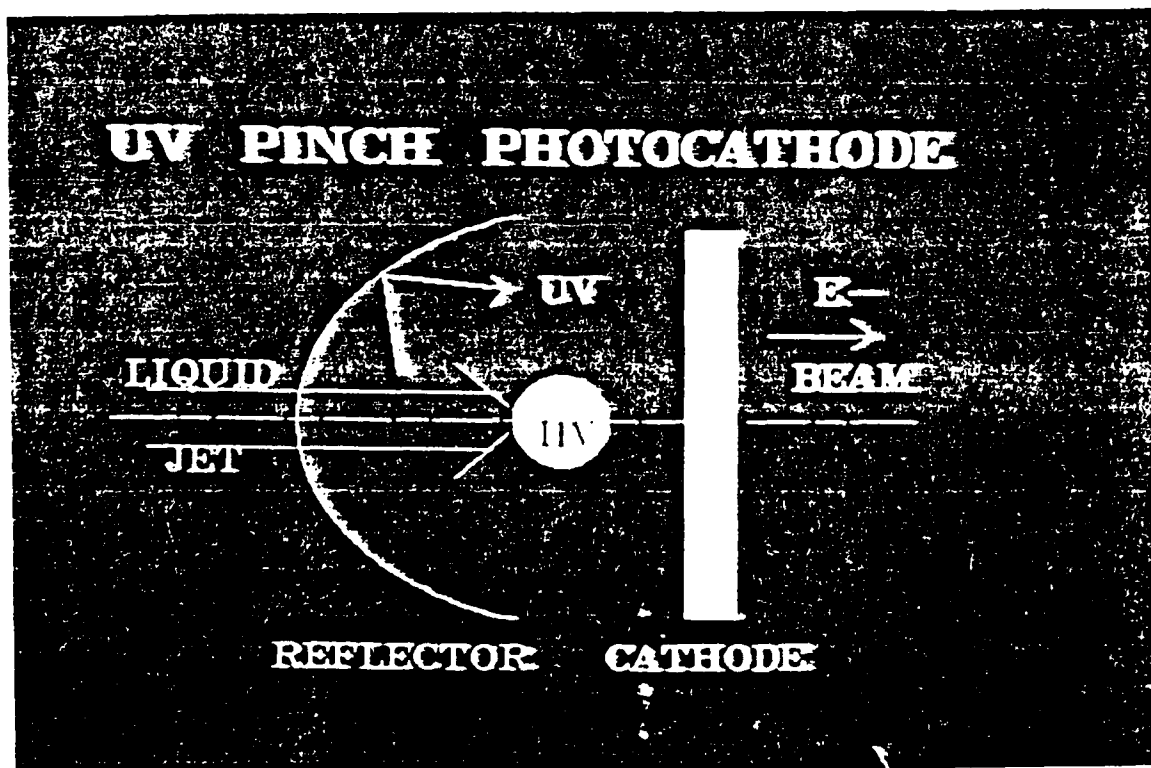


FIGURE 2. Schematic layout of the pinch photocathode apparatus.

reflector and the liquid jet. The circle labeled "HV" (High Voltage) represents the pinch discharge anode (where the cryogenic liquid trap is installed). It has a reentrant liquid sump from which the fluid is drawn from the system and collected in the trap.

A pseudocolor photograph of the liquid jet is shown at the top of Figure 3. The fluid is moving from left to right and two important phenomena are discernable. First, it can be seen that the diameter of the stream decreases with distance. Clearly, the fluid is evaporating, significantly. This verifies that a tenuous vapor cloud is forming around the jet as required to promote proper uniform preheating and initiation of the pinch. Second, it can be seen that the jet does not break up. Only at the end are there any indications of turbulence or hydrodynamic instability. The middle pseudocolor photograph (Figure 3) displays intensity contours for the radiation emerging from the pinch in the visible band. It is evident that the effective source size is many times larger than the liquid jet itself. Thus, it is clear that much of the visible emission is coming from the plasma generated in the plume region. On the other hand the bottom photograph of the sequence (depicting the UV emission) reveals a very compact source of dimension comparable to that of the dense jet itself. These observations lead us to conclude that the UV source is behaving essentially as desired.

Just as the above spatial observations yield insights as to the dynamics of the liquid-jet pinch, so, too, do the temporal data. The top trace of Figure 4 displays the visible output of the pinch as seen by the response of an S-20 calibrated planar

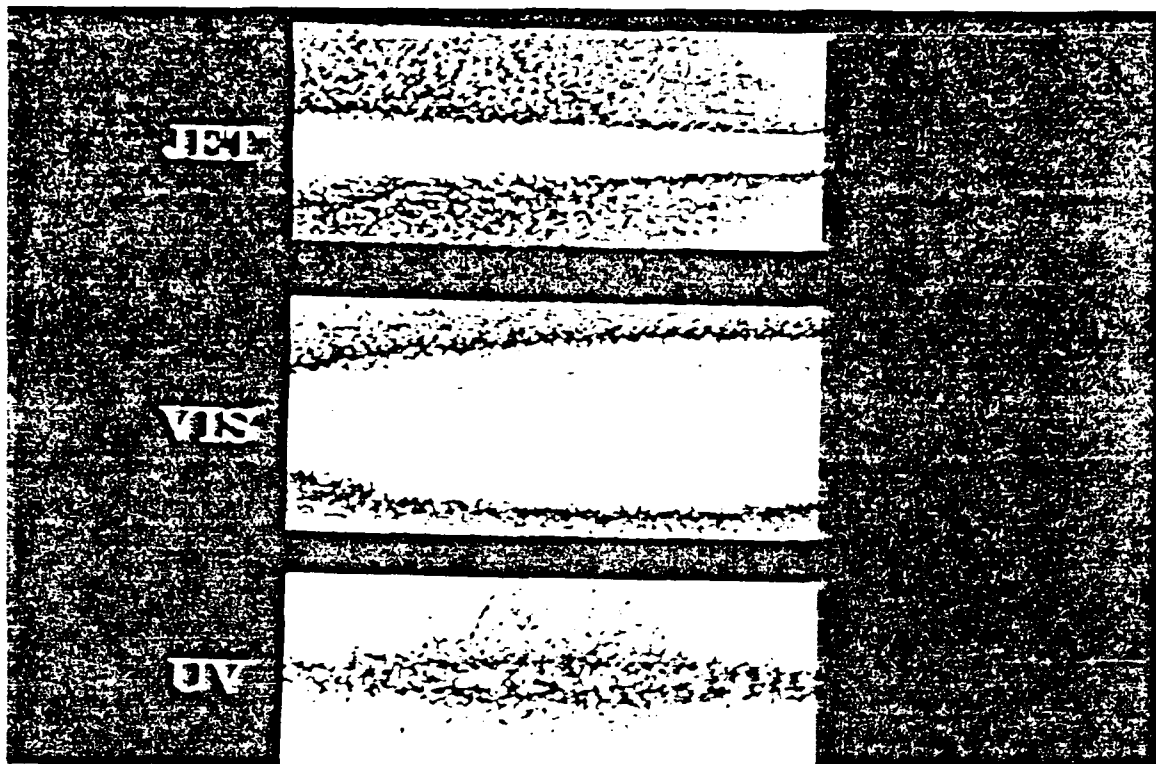


FIGURE 3. Pseudocolor photographs of the liquid jet (top), the visible radiation image of the plasma (center), and the ultraviolet image (bottom).

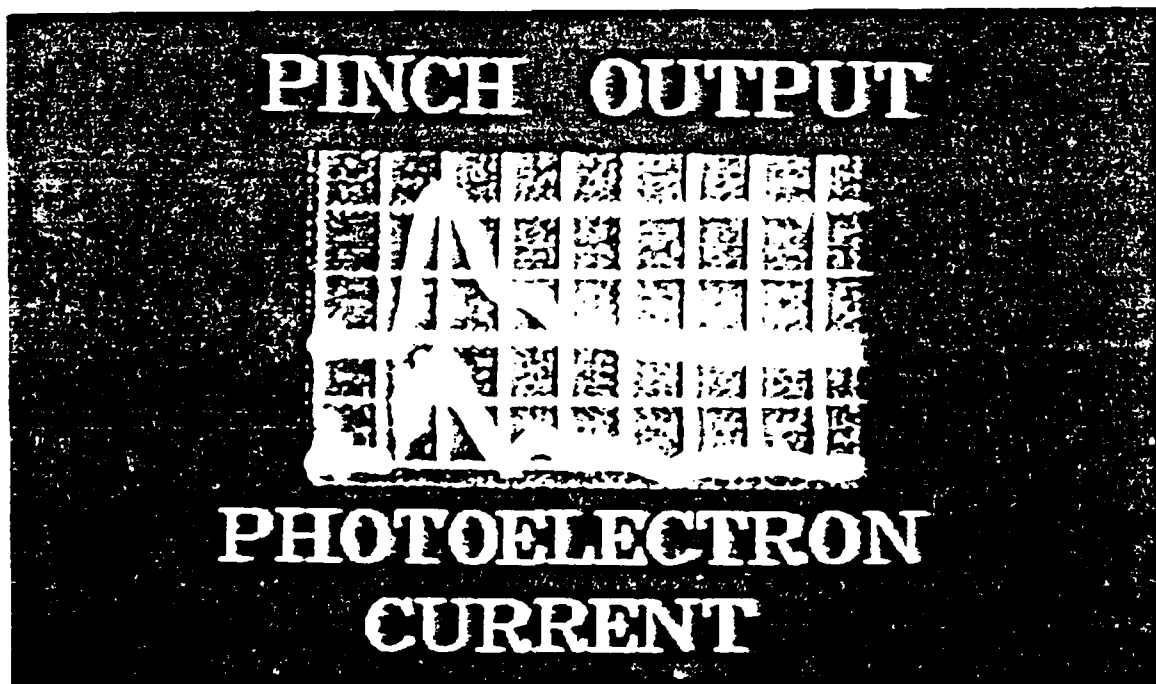


FIGURE 4. Visible radiation (top, $1 \mu\text{s/cm}$), and photocurrent.

photodiode. The bottom trace of this figure indicates the photoelectron current from the copper photocathode. As expected, it is a narrower pulse with a much higher ratio between the initial pulse and the late-time ringing of the PFN. This conforms with the expectation that the metal photocathode responds to hard UV and that hard UV is produced when the plasma is hottest (rather than when the plasma is at its greatest size). For comparison Figure 5 shows the predicted total radiation output of the pinch versus time as calculated by the radiation-hydro code developed earlier in the program.

The remaining two issues addressed with the present pinch apparatus are those of spectral content and rep-rate potential. In investigating the former we assembled a 1/4m spectrograph together with a 1700-element linear CCD multichannel analyzer. Spectral data were taken for a variety of radiation sources for comparison. These included our original gas-embedded pinch, the liquid-jet pinch, a surface flashover sparkboard, a pulsed laser, and a conventional xenon flashlamp. It emerged that the liquid-jet pinch produced the hardest radiation as well as a spectrum closest to the classical blackbody continuum. Figure 6 is a comparison of the spectrum of the pinch with that of the surface spark. From such evidence we conclude that the carefully tailored and balanced magnetic, inertial, and hydrodynamic forces effectively stabilize and contain the plasma so that it radiates as an optimal blackbody. Thus, it is compact and has a very high surface brightness so that it may be optically imaged to produce high-current photoemission.

The most recent issue addressed in the experimental work is

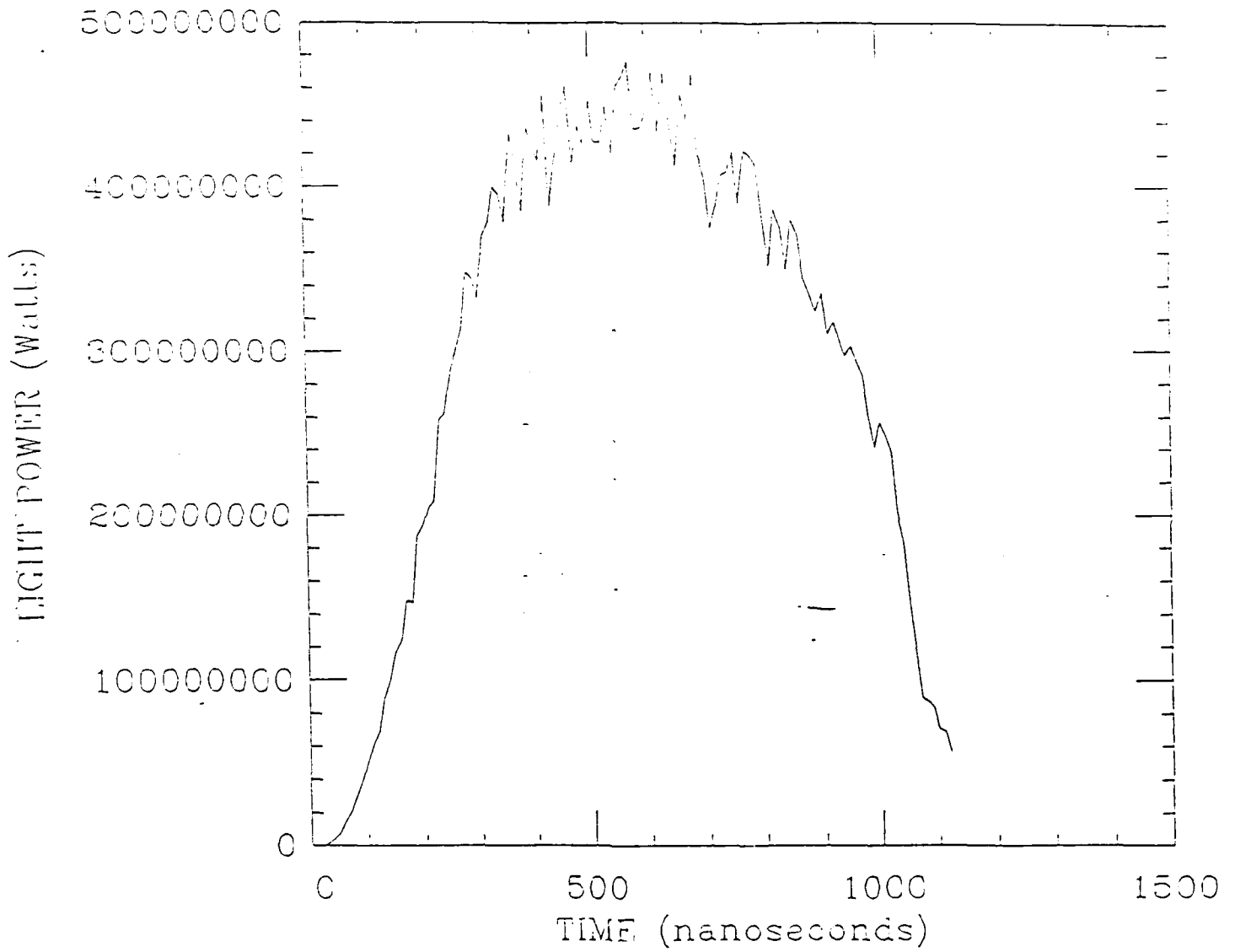


FIGURE 5. Radiation-hydro code calculation of the total radiation output versus time for the liquid-jet pinch.

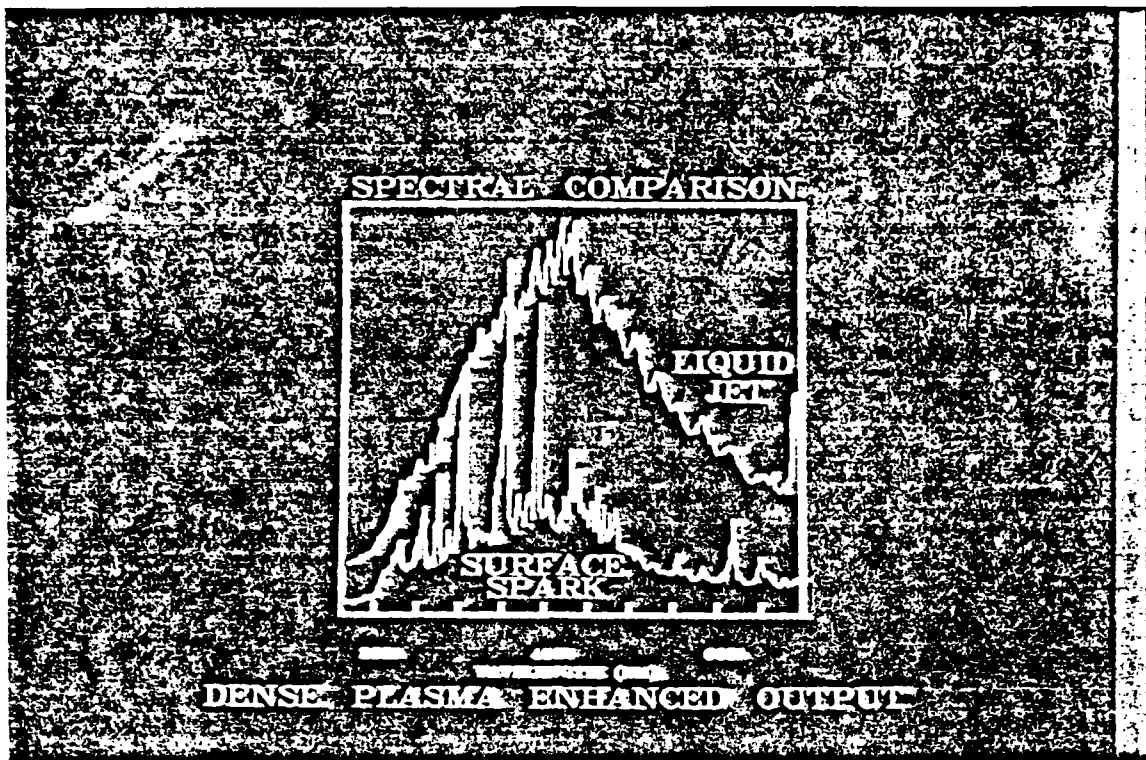


FIGURE 6. Raw spectra of the liquid-jet pinch and surface-spark UV sources.

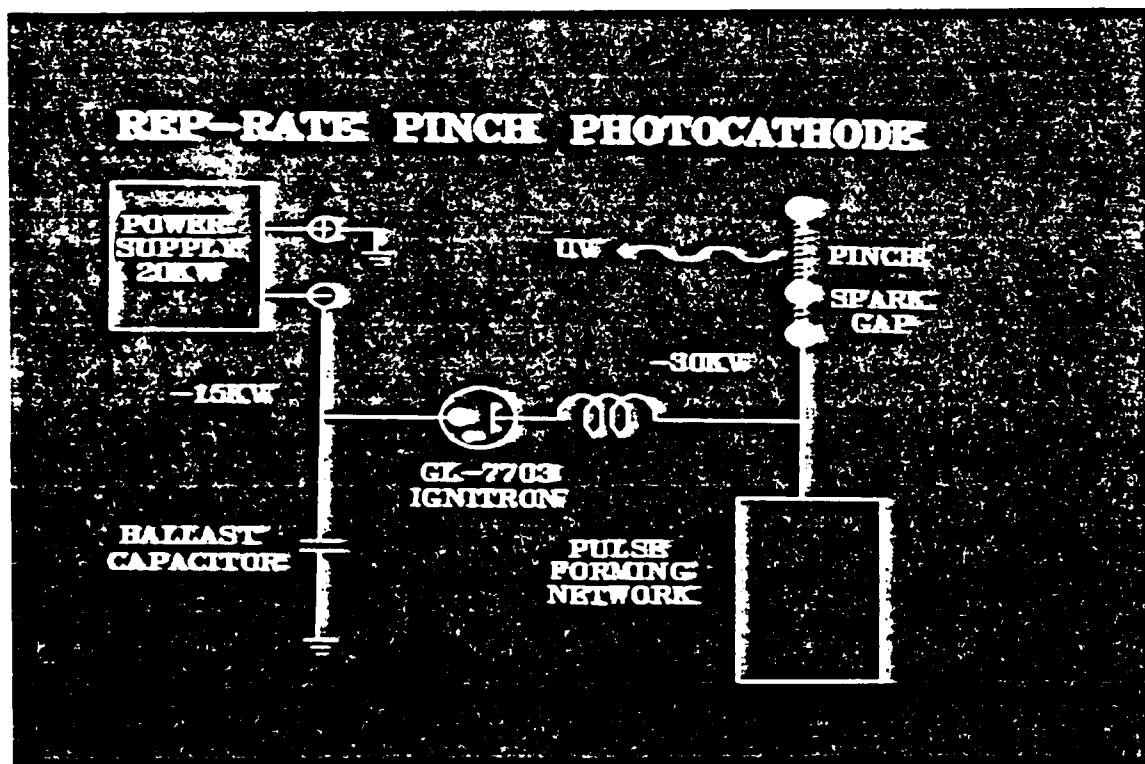


FIGURE 7. Schematic diagram of rep-rate pinch system.

that of the adaptability of the concept to rep-rate operation. In order to investigate this we have designed, built and tested a resonant pulse charging system to power the pinch photocathode system. It is shown schematically in Figure 7. Resonant voltage doubling is employed as the pinch requires 30 kV for proper operation, while our only high-power supply (20 kW) is limited to 20 kV. In addition the inductive isolation and lower-voltage supply yield a fail-safe configuration in terms of electrical fault protection (e.g., ignitron lock-on).

Initially, the pinch photocathode was operated at a 1 Hz rep rate without any changes to the system other than the pulse-charge power supply. Figure 8 shows the optical output of the rep-rate pinch as recorded by a Gentec fast calorimeter. The first two or three pulses are of nominal energy. However, the performance degrades quickly, thereafter. We determined that the chamber vacuum also degrades after the first shots. Evidently, only the first discharges are pinches and the later are diffuse involving the debris of the preceding shots that has not been removed by the pump. (The cryogenic cold trap was not employed in this decane-jet experiment.)

Subsequently, we enlarged and straightened the line to the vacuum pump and operated the cold trap with chilled flowing water. These measures improved the discharge performance as indicated by Figures 9 and 10. Figure 9 displays the waveforms for the first pulse of a ten-pulse train. The top two traces with a 1 ms sweep duration, monitor the pulse charging. The upper of these shows the PFN voltage dropping below the baseline to a full charge of -30 kV. The long time constant of the HV probe suggests

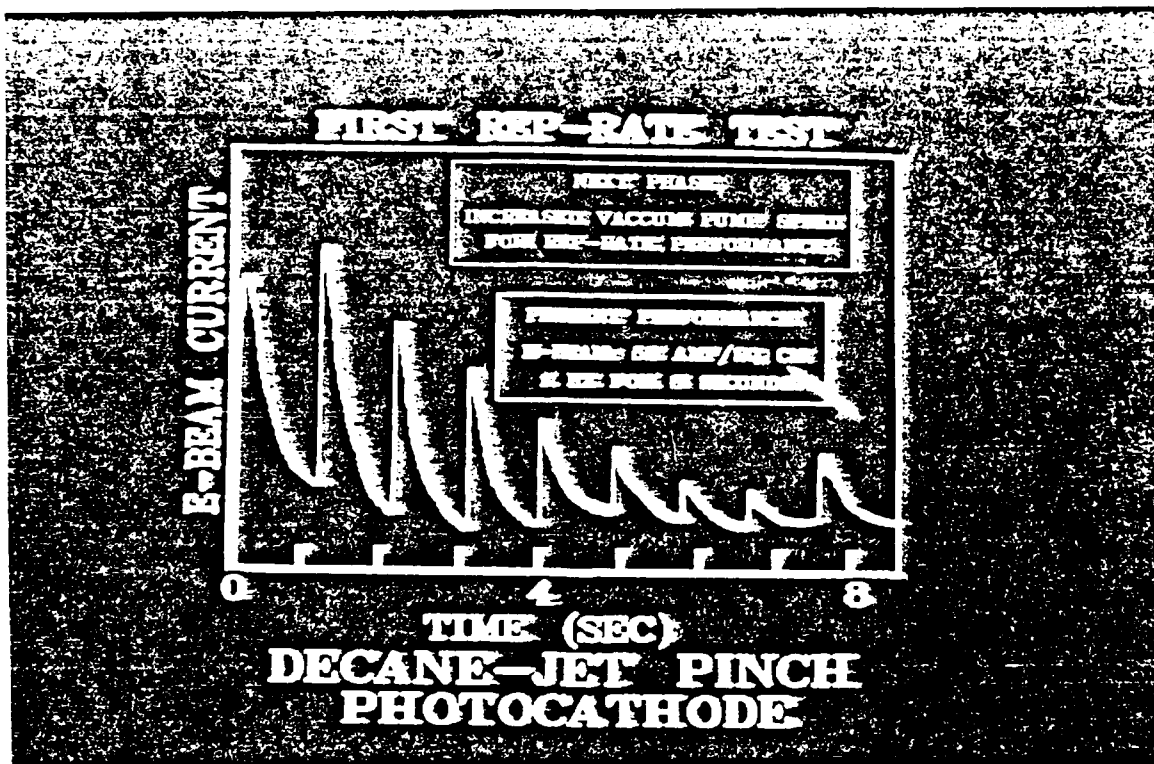


FIGURE 8. Rep-rate optical calorimeter output of the pinch.

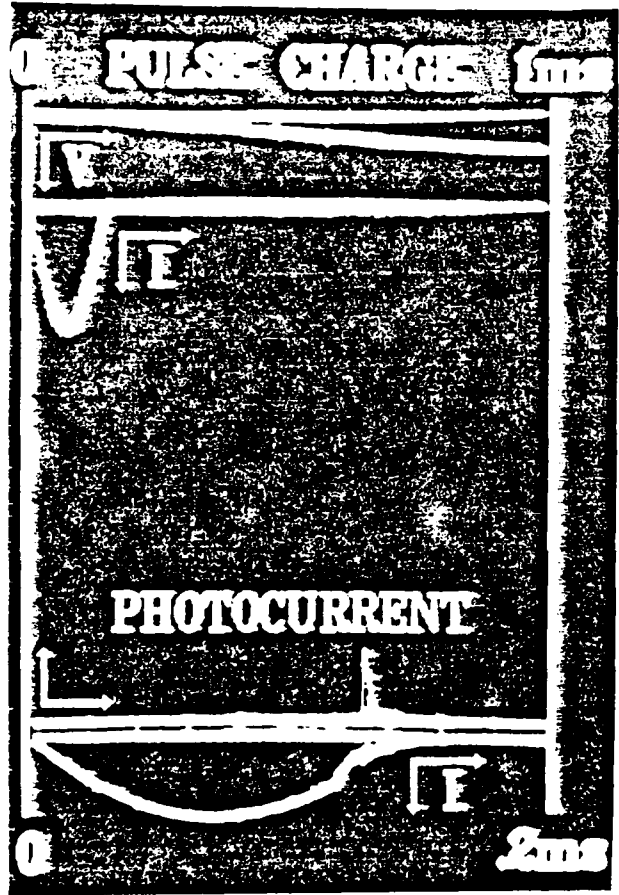


FIGURE 9. Performance of the pulse-charging system.

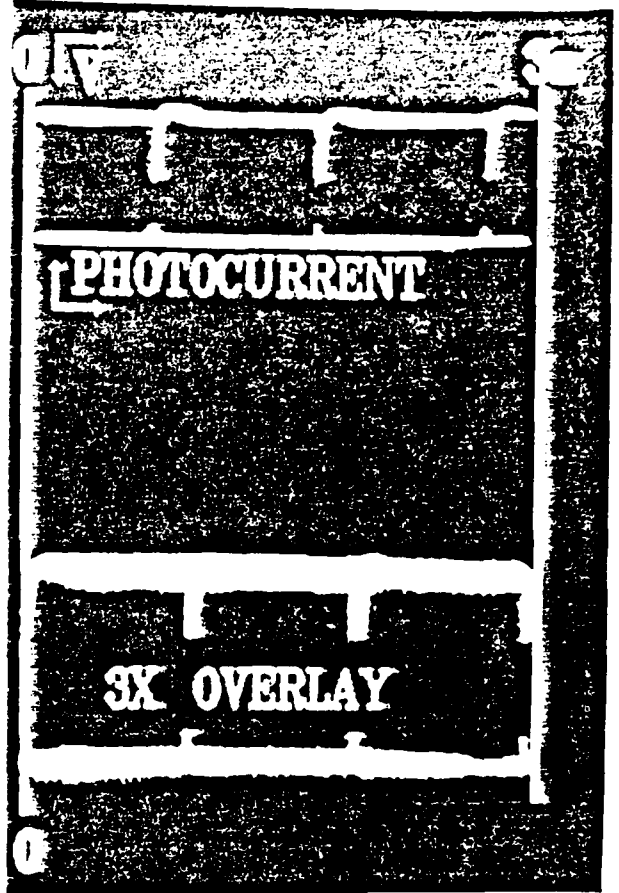


FIGURE 10. Rep-pulse behavior of the pinch photocathode

that this is taking 1 ms, whereas the charging duration is in fact 170 us. The 170 us charging current pulse is shown in the lower trace of both the upper and lower trace pairs at different sweep speeds. The upper trace of the lower pair labeled "photocurrent" is the output of the metal cathode photodiode. It occurs at the end of the charge cycle when the pinch is fired. Figure 10 displays the improved rep rate performance (to be compared with Figure 8) resulting from the higher vacuum pumping speed. In this figure the upper pair of traces display the repetitive pulse charge voltage and photocurrent for three pulses during a single three-second oscilloscope sweep. A three-sweep overlay displaying the 10 pulses of a 10-second run appears at the bottom of this figure. The system now runs reliably and reproducibly at 1 Hz. It has now been operated at 10 Hz, but with some erratic triggering that is being resolved.

A computer modeling effort has been underway since the beginning of the pinch photocathode effort. Initially, the code incorporated energy and momentum balance, Spitzer resistivity, and energy loss through blackbody radiation. In the past year multiple ionization and radiation transport have been included in an approximate way. This capability will be utilized to assist in the design of the ETA test photocathode described in the next section. To date all of the experimental work has been performed in the 1-3 us range of pulse duration. However, the ETA has a pulse duration of 0.1 us. Consequently, the computer modeling with this code will be helpful in making the transition. A typical 1 us code result was shown earlier (Figure 5).

3.0 PUBLICATIONS

1. Asmus, J.F. and R.H. Lovberg, "Dense-Pinch Photocathode", Proceedings of SPIE, 873 pp. 245-248 (13-15 January 1988).